IEEE Transactions on Nuclear Science, Vol. NS-28, No. 3, June 1981

MATCHING BUNCHED BEAMS TO ALTERNATING GRADIENT FOCUSING SYSTEMS*

Walter P. Lysenko
Los Alamos National Laboratory, Los Alamos, New Mexico 87545

Summary

A numerical procedure for generating phase-space distributions matched to alternating gradient focusing systems has been tested. For a smooth-focusing system a matched distribution can be calculated. With a particle tracing simulation code such a distribution can be followed while adiabatically deforming the focusing forces until an alternating gradient configuration is reached. The distribution remains matched; the final distribution is periodic with the structure period. External nonlinearities, including nonlinear couplings, were included in our examples but space charge was not. This procedure is expected to work with space charge but will require a 3-D space-charge calculation in the simulation code.

Introduction

In the smooth approximation in which the focusing forces are explicitly time independent, a phase-space distribution is said to be matched if it is constant in time. Such distributions can be formed by taking functions of the single-particle Hamiltonian (which can include space charge)

$$f(\vec{x},\vec{p}) \sim F\,[H(\vec{x},\vec{p})] \quad . \tag{1}$$

This procedure yields equilibria because the Hamiltonian is conserved for time-independent systems.

For periodic focusing systems a matched phase-space distribution is one that is periodic in time with the same period as the focusing forces. Because the forces are time dependent, Eq. (1) cannot be used. In the absence of any nonlinearities, matched distributions can be determined for periodic systems by the Courant-Snyder theory, which results in elliptical phase-space distributions. In this paper we present the test results for a method that includes nonlinear forces. Such matched distributions are obtained as follows. A distribution matched to a smooth-focusing system containing the axial nonlinearity and RF coupling terms is prepared by the numerical code RZED79, which uses Eq. (1). This distribution, represented by a collection of macroparticles, is followed in the particle tracing simulation code HOT while the focusing forces are adiabatically deformed until an alternating gradient configuration is reached. The distribution remains matched; it evolves from a time-independent distribution to one periodic with the structure period. An alternating gradient structure is three-dimensional and because the present HOT code does not have 3-D space-charge capabilities, the calculations were done without space charge. The new feature studied is the time dependence of the forces. Space-charge forces or other features of the focusing forces could be included in the particle tracing code, and distributions matched to the new situation should result.

Distributions Matched to Smooth-Focusing Systems

Distributions matched to a smooth-focusing system were generated using Eq. (1) with the following choice for the function F

$$F(H) \sim \begin{cases} H_0 - H, & H_0 - H \quad 0 \\ 0 \quad , & H_0 - H > 0 \end{cases} \tag{2}$$

in which H_0 is a constant. This is one of the functions used in the one-degree-of-freedom work by Gluckstern, Chasman, and Crandall.[1] In the present case we use a two-degree-of-freedom, r-z Hamiltonian to describe the nonrelativistic single-particle motion.

$$H(\vec{x},\vec{p}) = \frac{1}{2m} p^2 + \frac{k}{2} r^2 + \frac{k_z}{2} z^2 - \frac{\pi k_z \cot\phi_s}{3\beta\lambda} z^3 \tag{3}$$

$$+ \frac{\pi k_z \cot \phi_s}{2\beta\lambda} r^2 z + e\phi(r,z)$$

The coordinates $\vec{x}$ and momenta $\vec{p}$ are relative to the synchronous particle with $r^2 = x^2 + y^2$ and $p^2 = p_x^2 + p_y^2 + p_z^2$. The synchronous phase is ϕ_s and the space-charge potential is $\phi(r,z)$. Except for the axial nonlinearity term (z^3) and the RF coupling term ($r^2 z$), the method for producing a matched distribution using the RZED code (RZED79 is the nonlinear version) has been previously described.[2] With no space charge ($\phi = 0$), the procedure is straightforward.

We started with a beam matched to a $2\beta\lambda$ drift-tube linear accelerator, assuming smooth focusing with a phase advance of 90° per focusing period in all directions. We chose a large beam emittance to more clearly see nonlinear effects. To further enhance nonlinear effects the initial beam was traced for 20 focusing periods while increasing the focusing strengths of the smooth-focusing forces so that the final phase advances were 108° in all three directions. This new "initial" beam was then used as the starting point in the experiment to generate the time-dependent matched beam. The 108° tune is near the nonlinear $2\sigma_x + \sigma_z = 360°$ resonance so that matching to the nonlinearity becomes more important.

Parameter Variation in Particle Tracing

Figure 1 shows the strengths of the linear parts of the focusing forces in the three directions over one focusing period (four RF cycles). The focusing strengths are expressed in terms of instantaneous phase advances per focusing period. A negative value for the instantaneous phase advance means the force defocuses. The focusing period in Fig. 1 starts with an x-defocusing lens, followed by a drift, followed by an x-focusing lens, followed by a second drift. The lens lengths are $\beta\lambda$. At the centers of the drifts are RF gaps of length $\beta\lambda/4$.

The alternating gradient configuration is achieved as follows. In the first focusing period of the simulation, the focusing strengths are constant over the period. In subsequent focusing periods, the focusing strength in the x-direction is decreased in the x-defocusing lens region and increased in the x-focusing lens region so that the instantaneous phase advances in these regions are some new values σ_1 and σ_2, respectively. In the drifts between the lenses, the focusing strength is set so that the instantaneous phase advance there is $(\sigma_1 + \sigma_2)/2$; in the y-direction, they are set so that the instantaneous phase advances are σ_2, σ_1, and $(\sigma_1 + \sigma_2)/2$ in the three regions, respectively. In the z-direction, the instantaneous phase advance in the gap region is increased and the instantaneous phase advance in the region between the gaps is decreased. At every focusing period, the strengths are changed by a small amount until finally σ_1 and σ_2 are equal in magnitude but opposite in sign, and the drifts contain no transverse forces. In the axial direction, the final configuration has forces confined to the gap region.

*Work performed under the auspices of the U. S. Department of Energy.

0018-9499/81/0600-2516$00.75©1981 IEEE

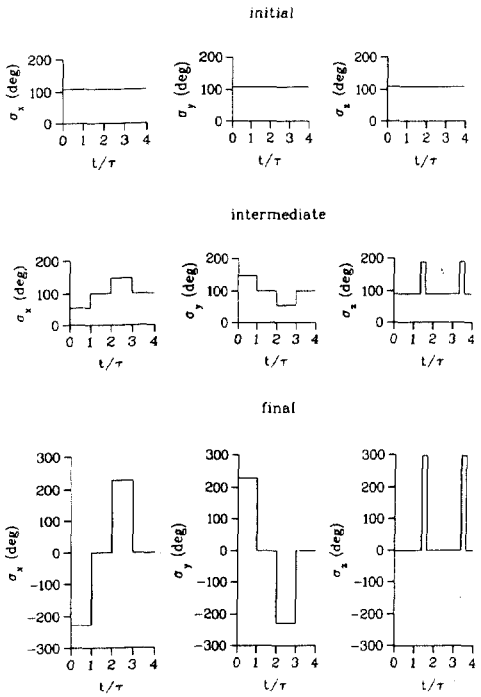

Fig. 1. The focusing strengths in the three directions are shown as functions of time over one focusing period for the initial, an intermediate, and the final configuration. The phase advance per period is always 108° in all directions.

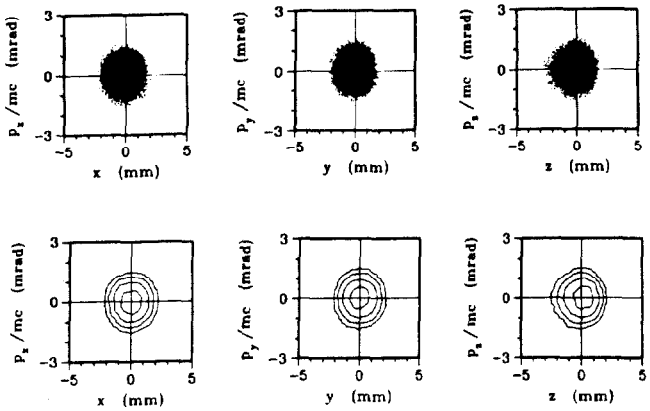

Fig. 2. Matched beam at focusing period number 20. The structure at this point is smooth focusing with phase advances per period of 108° in all directions. The scatter plots show the projections of the six-dimensional phase-space coordinates of the 10 000 macroparticles onto the two-dimensional phase-space planes. The contour plots show contours of equal density of points in the two-dimensional projections. The contours show densities of 0.7, 0.3, 0.1, and 0.02 in units of the maximum density.

Particle Tracing Results

The initial matched phase-space distribution was represented in HOT by 10 000 macroparticles. Figure 2a shows the three 2-D phase-space projections at focusing period 20, where the focusing forces are still smooth. Figure 2b shows the contours of equal density in the same phase planes. The contours represent densities of 0.7, 0.3, 0.1, and 0.02 in units of the maximum phase-space density. The axial phase-space shape is not elliptical because the beam is matched to the very nonlinear axial forces. This distribution was traced from this point with acceleration still turned off while bringing the focusing forces to the final alternating gradient configuration in 100 focusing periods. The phase advance per period was maintained at 108° in all directions. At period number 120, the final alternating gradient configuration is reached and the accelerator parameters are held fixed as the distribution is followed for 20 more focusing periods. Figures 3 and 4 show the contour plots at focusing period 121 and 126, respectively. The distributions, at times an integral number of focusing periods apart, are very similar. This is the desired result: the distribution is periodic.

Because the phase-space projections are not elliptical, the usual ellipse-fitting, area-measurement procedure is not adequate. We used a bin-counting procedure, which was less shape dependent. The statistical error in the 98% bin-counting emittance of the initial beam of 10 000 macroparticles is 1.3%.

There are fluctuations in the 98% emittance of ±3.5% (large emittance in the defocusing lens and small in the focusing lens). Emittance values, at times an integral number of periods apart, are more nearly constant. The worst point in the 20 periods was at the x-defocusing lens in period 134, for which the emittance was 3.0% higher than at the corresponding point of period 121. Because the emittance is approximately periodic, the emittance averaged over a period is nearly constant. The 98% emittance averaged in this way varies at most by +2.3%, at period 134, from the average at period 121. Another kind of average, even more constant, is the 98% emittance averaged over the three directions x, y, and z. Averaged this way, the fluctuations over a period almost disappear. All 80 values of $(\eta_x + \eta_y + \eta_z)/3$ over the 20 periods lie in the interval 2.80 mm·mrad ± 0.9%. This is an experimental result that could not have been predicted because, for more than one degree of freedom, there is no known conservation law involving the emittances.

Figure 5 shows the time evolution of the rms emittance in the x-direction. The general behavior of the rms emittance is similar to that of the 98% emittance. The fluctuations are smaller (±2.4%) and the maximum change in the emittance averaged over a period is smaller (+1.2%). For a linear uncoupled system, the rms emittance is conserved for any distribution, even a mismatched one. The observed fluctuations are therefore caused by the nonlinearities.

For comparison, a uniformly filled ellipsoid in 6-D phase space was prepared with the Courant-Snyder parameters chosen to match to the linear part of the focusing forces. Because the nonlinearities were not considered in preparing the uniform distribution, there is a mismatch. Figure 5 shows also the results for the uniform beam.

The uniform beam's time evolution can be understood to some degree because the tune is near the $2\sigma_x + \sigma_z = 360°$ resonance. This resonance is excited in the first harmonic of the RF coupling potential. Because RF coupling is included in our model and because the beam is large, we expect this effect to be large. The resonant combination of phase advances is 36°; that is, $2\sigma_x + \sigma_z - 360° = 36°$. According to first-order perturbation theory, the amplitudes of the oscillation in the x- and z-directions should oscillate with a period of 10 focusing periods (360°/36°). Because of the spread of phases, we expect the emittance in both the x- and z-directions to increase. After 10 focusing periods we expect the distribution to return to its original form because it was matched to the

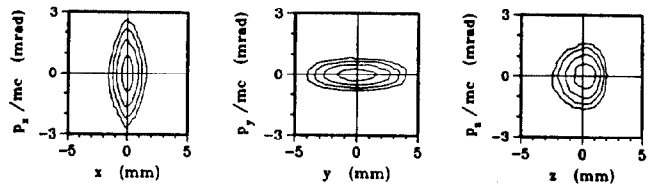

(a) at center of x-defocusing lens

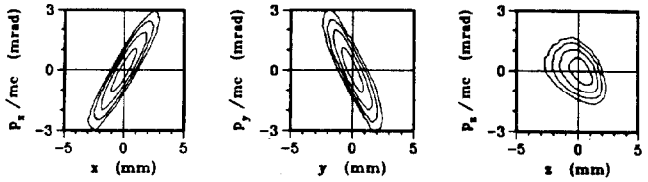

(b) at exit of first RF gap

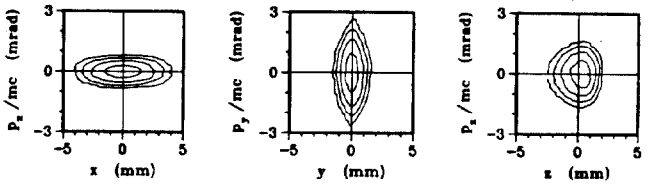

(c) at center of x-focusing lens

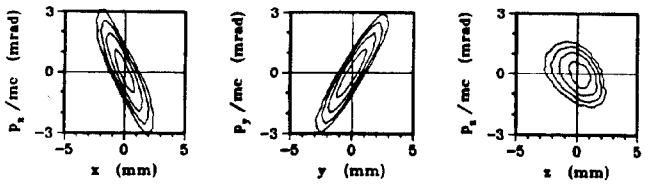

(d) at exit of second RF gap

Fig. 3. Contour plots for matched beam at focusing period number 121.

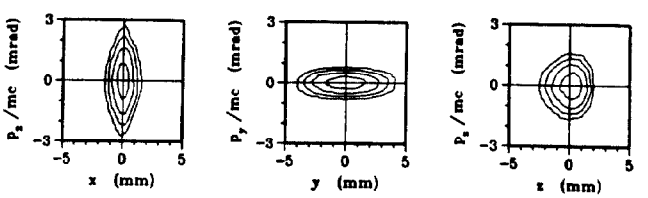

(a) at center of x-defocusing lens

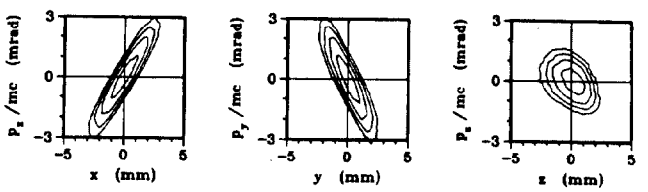

(b) at exit of first RF gap

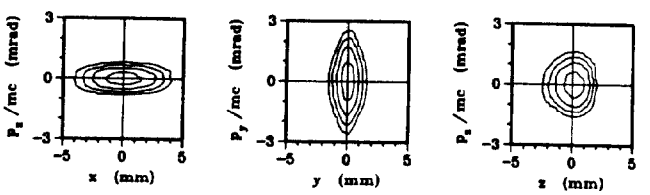

(c) at center of x-focusing lens

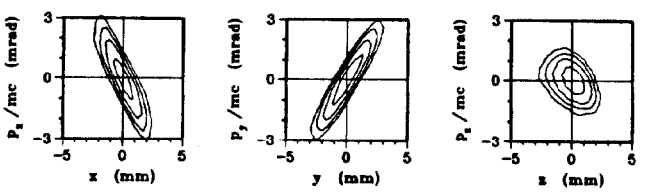

(d) at exit of second RF gap

Fig. 4. Contour plots for matched beam at focusing period number 126. Note that corresponding phase-space projections are similar to those in Fig. 3.

linear forces. But because the perturbation theory result is not exact, there is some average emittance growth.

Discussion

We have tested the following procedure. To produce a phase-space distribution that is matched to a given structure, we start with a structure for which an equilibrium distribution is known and deform the structure adiabatically into the desired structure, following the distribution with a particle tracing code. Our example shows that we can obtain a distribution matched to an alternating gradient focusing structure, including the axial nonlinearity and nonlinear RF coupling forces, starting from a distribution matched to an azimuthally symmetric, smooth-focusing structure. This procedure resulted in a periodic distribution even though the beam was large and the tune was near a nonlinear resonance, which led to nonelliptical phase-space shapes. This matched distribution did not exhibit the emittance growth that occurred for an elliptical distribution with the Courant-Snyder parameters determined by the linear parts of the focusing forces. This result is encouraging because if it still works with space charge in the future 3-D particle tracing code, it means we will have distributions matched to a very realistic model of the accelerator.

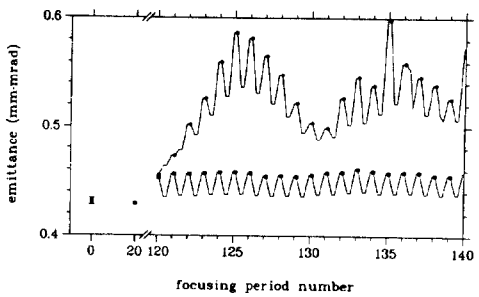

Fig. 5. The rms emittance in the x-direction as a function of the focusing period number. The lower curve is the matched beam and the upper curve is the uniform-in-six-dimensional-phase-space beam.

References

1. R. L. Gluckstern, R. Chasman, and K. Crandall, "Stability of Phase-Space Distributions in Two-Dimensional Beams," Proc. 1970 Proton Linear Accelerator Conf., National Accelerator Laboratory, 1970, p. 823.

2. W. P. Lysenko, "Equilibrium Phase-Space Distributions and Space-Charge Limits in Linacs," Los Alamos report LA-7010-MS (October 1977).